

# Wide-view and sunlight readable transfective liquid-crystal display for mobile applications

Zhibing Ge,<sup>1</sup> Shin-Tson Wu,<sup>1,\*</sup> and Seung Hee Lee<sup>2</sup>

<sup>1</sup>College of Optics and Photonics, University of Central Florida, Orlando, Florida 32816, USA

<sup>2</sup>Department of Polymer Nano-Science and Engineering, Chonbuk National University, Chonju, Chonbuk 561-756, Korea

\*Corresponding author: swu@creol.ucf.edu

Received July 18, 2008; revised September 28, 2008; accepted October 1, 2008; posted October 13, 2008 (Doc. ID 98849); published November 11, 2008

A wide-view single cell gap transfective liquid-crystal display (TR-LCD) using the fringe field switching effect is proposed by incorporating a quarter-wave in-cell-retarder below the liquid-crystal (LC) cell in the reflective part. By optimizing the angle between the electrode stripes and the LC rubbing direction in the transmissive and the reflective regions, this TR-LCD exhibits a high optical efficiency and good match between the voltage-dependent transmittance and reflectance curves. Without using any phase compensation films, this TR-LCD exhibits a wide view with 10:1 contrast ratio over a 60° viewing cone in the transmissive mode and over a 40° cone in the reflective mode, which is adequate for mobile displays. © 2008 Optical Society of America

OCIS codes: 230.3720, 230.2090.

A wide-view transfective liquid-crystal display (TR-LCD) [1,2] has been widely used for mobile displays because of its sunlight readability and low power consumption. To balance the optical path-length disparity between the transmissive (T) and reflective (R) regions, most TR-LCDs adopt a dual cell gap configuration [1,3]. Although the dual cell gap approach leads to a good gray scale overlapping between the voltage-dependent transmittance (VT) and voltage-dependent reflectance (VR) curves, it complicates the fabrication process and degrades the contrast ratio near the T-R boundaries. In addition, to obtain a good dark state of the R mode, circular polarizers (CPs) are commonly used in both T and R regions, which results in a narrow viewing angle [4,5]. Thus, in-plane switching (IPS) and fringe-field switching (FFS) based TR-LCDs that inherently have a wide viewing angle for the T mode under two linear polarizers (LPs) are getting more research attention [6–13]. For IPS and FFS based TR-LCDs, the major challenge is to obtain a normally black R mode because the liquid crystals (LCs) are initially aligned parallel or perpendicular to the top LP's transmission axis.

One way to solve this problem is to use an in-cell-retarder (ICR). By inserting a half-wave ( $\lambda/2$ ) ICR above the  $\lambda/4$  LC cell in the R region [7], the top LP,  $\lambda/2$  ICR, and  $\lambda/4$  reflective LC layer together form a broadband CP for achieving a normally black state for the R region. However, under this design different cell gaps between T and R regions are still required, and the obtained reflectance is relatively low. Another approach is to use a patterned  $\lambda/4$  phase retarder merely in the R region. Thus, the top LP and ICR jointly form a CP [8,9]. For the ICR embedded TR-LCDs, FFS mode is preferred to the conventional IPS because in the FFS structure the metal reflector can be shielded by the plane common electrode to minimize its influence on the fields in the LC cell. However, in [9] the ICR is formed directly in the LC

layer of the R region, which is equivalent to have a dual cell gap structure so that the contrast ratio degradation near the T–R boundaries still exists. Besides, the ICR formed above the electrodes also greatly shields the electric fields in the R part, resulting in an increased driving voltage and unmatched VT and VR curves. Yet another approach is to insert a uniform  $\lambda/4$  ICR below the LCs in both T and R regions for a single cell gap, but an additional compensation film below the reflector is needed to cancel the ICR in the T region [10,11]. Its major drawback is that the T mode loses its inherent wide-viewing angle after including the ICR and compensation film. Therefore, there is an urgent need to develop a wide-view single cell gap FFS TR-LCD with a single gamma curve and low operating voltage.

In this Letter, we propose an FFS TR-LCD by incorporating a  $\lambda/4$  ICR below the driving electrodes in the R region. This FFS TR-LCD maintains a truly single cell gap and an inherent wide-view T mode. Moreover, the ICR and the reflector do not affect the driving voltage of the R part, leading to a low driving voltage. By optimizing the angle between pixel electrode stripes and the LC rubbing direction in both T and R regions, the maximum light efficiency of T and R modes using a  $+\Delta\epsilon$  LC material reaches  $\sim 83\%$  and  $86\%$ , respectively. Besides, the VT and VR curves match well, which enables single gamma curve driving.

Figures 1(a) and 1(b) show the electrode layout and a cross section of the proposed device structure. Each LC pixel is divided into separate T and R regions, which are driven by patterned pixel electrodes and a plane common electrode that are formed on the same bottom substrate. Throughout the whole cell, the LC directors are initially homogeneously aligned with their optic axis parallel to the top LP's transmission axis [at about  $-57.5^\circ$  as shown in Fig. 1(a)]. The bottom LP has its transmission axis set perpendicular to the top one for a good dark state of the T mode. In the

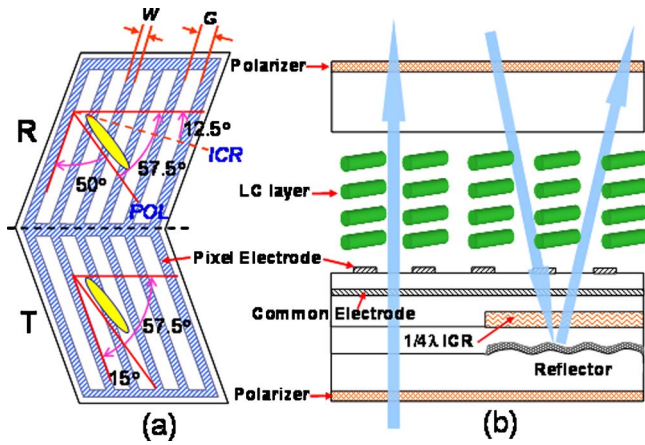


Fig. 1. (Color online) Device structure of the single cell gap FFS transfective LCD device.

R part, below the common electrode, a  $\lambda/4$  ICR is formed above the reflector with its optic axis at about  $45^\circ$  away from the transmission axis of the top LP. Thus the top LP and the ICR form a CP for getting a normally black R mode. In this configuration, both ICR and metal reflector are shielded by the common electrode, thus they do not affect the fields from the driving pixel and common electrodes, making a low operating voltage attainable by a proper LC material selection and electrode design. In addition, to obtain a high optical efficiency and matched VT and VR curves, the pixel electrode stripes in the T and R regions are set at about  $15^\circ$  and  $50^\circ$  away from the LC rubbing direction, respectively.

Figure 2 shows the optical configuration for this TR-LCD. When no voltage is applied, the LC directors are all initially aligned parallel to the transmission axis of the top LP. Hence, in the T part the light from the bottom LP retains its polarization after traversing the LC layer and is then blocked by the top LP. In the R part, the optic axes of the LC cell and the  $\lambda/4$  ICR are set at  $0^\circ$  and  $45^\circ$  with respect to the top LP's transmission axis, respectively. Thus, the ICR and the top LP form a CP to warrant a common dark state for the R mode.

On the other hand, as the applied voltage well exceeds the threshold voltage, the LC directors are re-oriented by the electric fields. Here as shown in Fig. 1(a), in the T part, the stripe pixel electrodes are

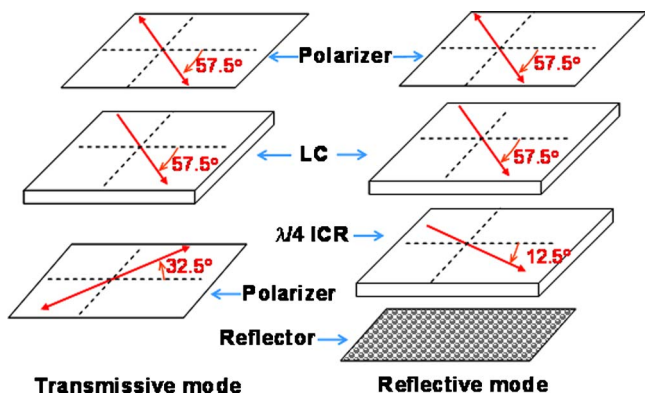


Fig. 2. (Color online) Optical configuration of the T and R modes at a dark (voltage-off) state.

formed with an angle of about  $15^\circ$  with respect to the LC rubbing direction to gain an optimal rotation. Under proper reorientation (its effective optic axis is about  $45^\circ$  away from its initial orientation), the LC cell can be tuned to be functionally equivalent to a  $\lambda/2$  plate to rotate the bottom incident light by  $90^\circ$  for a high transmittance. In the R part, the mechanism to obtain a high reflectance is slightly more complicated. From Fig. 2, it has two requirements: (1) the on-state reflective LC cell needs to be functionally equivalent to a  $\lambda/2$  plate and (2) the on-state LC effective optic axis in the R part should be about  $22.5^\circ$  away from the top LP transmission axis. Thus the incident linearly polarized light from the top LP will be rotated by  $45^\circ$  by the R LC cell to become parallel to the optic axis of the ICR. As a result, the ICR will not change the polarization of the light passing through it, and the reflected light remains its linear polarization again when traversing the ICR layer and then experiences a second polarization rotation by the LC layer that makes its final polarization along the top LP's transmission axis for a maximum reflectance. From the above analysis, we can see that both T and R regions require the LC cell to function as a  $\lambda/2$  plate for an optimum light output, thus a truly single cell gap can be obtained. In addition, the required rotation angle of the LC layer in the T and R regions are different, resulting in a different pixel electrode stripe orientation in these two regions.

To validate this device concept and investigate its performance, the electro-optic performance of this device is calculated using commercial software 2DIMMOS (from Autronic-Melchers, Germany) for the LC director distribution and the  $2 \times 2$  matrix method [14,15] for the optical characterization thereafter. A  $+\Delta\epsilon$  LC mixture is employed with its physical properties listed as follows: elastic constants  $K_{11}=9.7$  pN,  $K_{22}=5.2$  pN, and  $K_{33}=13.3$  pN, dielectric anisotropy  $\Delta\epsilon = +8.2$ , birefringence  $\Delta n=0.1$  at  $\lambda=550$  nm, and rotational viscosity  $\gamma=84$  mPa s, and the FFS cell has a uniform cell gap of  $3.5 \mu\text{m}$  with a surface pretilt angle of  $2^\circ$ . The ICR has a birefringence about  $\Delta n=0.17$  at  $\lambda=550$  nm and a thickness of  $0.809 \mu\text{m}$  [16]. As shown in Fig. 1(a), the pixel electrode stripes have an angle of about  $15^\circ$  and  $50^\circ$  with respect to the LC rubbing direction in the T and R regions, respectively. Here the pixel electrode width (W) and gap (G) in both T and R regions are set at 3 and 4  $\mu\text{m}$ , respectively.

Figure 3 shows the calculated VT and VR curves, where a maximum transmittance of  $\sim 28\%$  and a maximum reflectance of  $\sim 29\%$  are both obtained at  $V=4.5 V_{\text{rms}}$ . Here the maximum possible light output from two parallel LPs is  $\sim 33.7\%$ . The reduced light efficiency of the T and R modes results from two factors: (1) when a  $+\Delta\epsilon$  LC material is used, besides an in-plane rotation, the LC directors near the electrode surface will also be tilted by the fringe fields, leading to a lower phase retardation and (2) in the bright state, the LC rotations along the vertical cell direction are not uniform at different horizontal cell positions (e.g., rotation angle peaks near the electrode edges and minimizes near the centers of the elec-

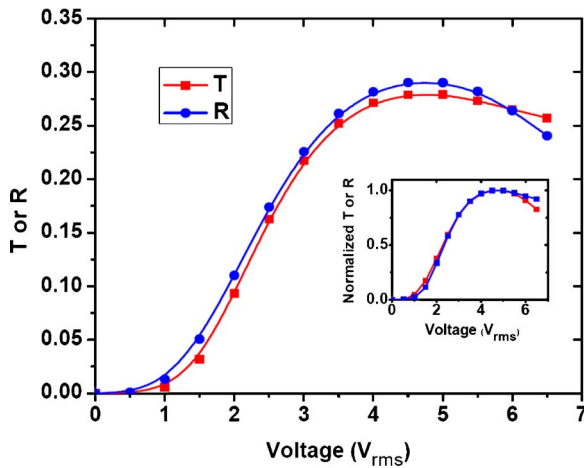


Fig. 3. (Color online) VT and VR curves for this display (inset plots show the normalized results) at  $\lambda=550$  nm.

trodes or slits). In other words, not every position can work as an effective  $\lambda/2$  plate [17]. Aside from obtaining a high light output, the angles between the electrode stripes and the LC rubbing direction in both T and R regions are also selected for achieving a good overlap between the VT and VR curves. The normalized VT and VR curves exhibit an excellent match as shown in the inset of Fig. 3, which indicates that a single gray scale driving circuit can be employed for this display.

In addition to high optical efficiency, a wide-viewing angle is also critical for mobile displays. The iso-contrast plots are shown in Fig. 4(a) for the T mode and in Fig. 4(b) for the R mode, respectively. As expected, the T mode shows an inherently wide-viewing angle with its CR > 10:1 viewing cone over  $60^\circ$  at every direction. For the reflective mode, the CR > 10:1 is over a  $40^\circ$  viewing cone, which is typical in such a single CP configuration (LP and a  $\lambda/4$  ICR). In all, these viewing angles are adequate for mobile

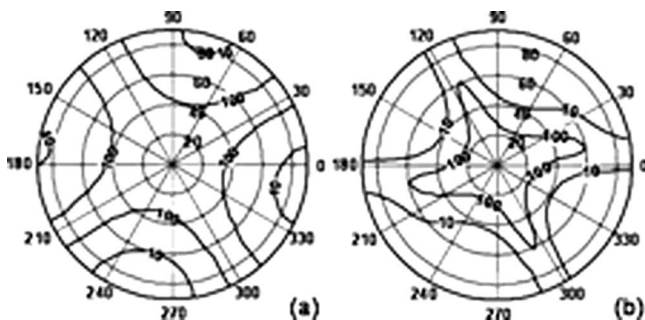


Fig. 4. Iso-contrast plots for (a) T mode and (b) R mode of this display at  $\lambda=550$  nm.

displays using a small LCD panel. In addition, the FFS modes exhibit a smaller off-axis color change as compared to other LC modes like the VA mode [18], making it attractive for mobile displays.

In conclusion, we have developed an FFS based TR-LCD that provides a low driving voltage single cell gap by incorporating an ICR below the common electrode of the reflective LC part. This TR-LCD also shows well matched VT and VR curves, making it suitable for one gamma curve driving. Moreover, this TR-LCD exhibits a wide-viewing angle for the T mode and a reasonably good viewing angle for the R mode. We believe this design has a great application potential for future high performance mobile LCDs.

The authors are indebted to the financial support from Chi-Mei Optoelectronics, Taiwan.

## References

1. For a review, X. Zhu, Z. Ge, T. X. Wu, and S. T. Wu, *J. Disp. Technol.* **1**, 15 (2005).
2. A. K. Bhowmik, Z. Li, and P. J. Bos, *Mobile Displays* (Wiley, 2008).
3. M. Okamoto, H. Hiraki, and S. Mitsui, U.S. patent 6,281,952 (August 28, 2001).
4. S. Pancharatnam, *Proc. Indian Acad. Sci. Sect. A* **41**, 130 (1955).
5. Z. Ge, M. Jiao, R. Lu, T. X. Wu, S. T. Wu, W. Y. Li, and C. K. Wei, *J. Disp. Technol.* **4**, 129 (2008).
6. S. H. Lee, S. L. Lee, and H. Y. Kim, *Appl. Phys. Lett.* **73**, 2881 (1998).
7. H. Imayama, J. Tanno, K. Igeta, M. Morimoto, S. Komura, T. Nagata, O. Itou, and S. Hirota, *Soc. Inf. Disp. Tech. Digest* **38**, 1651 (2007).
8. J. B. Park, H. Y. Kim, Y. H. Jeong, S. Y. Kim, and Y. J. Lim, *Jpn. J. Appl. Phys. Part 1* **44**, 7524 (2005).
9. G. S. Lee, J. C. Kim, T.-H. Yoon, Y. S. Kim, W. S. Kang, and S. I. Park, in *Proceedings of the 26th International Display Research Conference* (Society for Information Display, 2006), p. 75.
10. J. H. Song, Y. J. Lim, M. H. Lee, S. H. Lee, and S. T. Shin, *Appl. Phys. Lett.* **87**, 011108 (2005).
11. Y. J. Lim, M. H. Lee, G. D. Lee, W. G. Jang, and S. H. Lee, *J. Phys. D* **40**, 2759 (2007).
12. H. Y. Kim, Z. Ge, S. T. Wu, and S. H. Lee, *Appl. Phys. Lett.* **91**, 231108 (2007).
13. Z. Ge, T. X. Wu, and S. T. Wu, *Appl. Phys. Lett.* **92**, 051109 (2008).
14. A. Lien, *Appl. Phys. Lett.* **57**, 2767 (1990).
15. Z. Ge, X. Zhu, T. X. Wu, and S. T. Wu, *J. Opt. Soc. Am. A* **22**, 966 (2005).
16. H. Hasebe, Y. Kuwana, H. Nakata, O. Yamazaki, K. Takeuchi, and H. Takatsu, *Soc. Inf. Disp. Tech. Digest* **39**, 1904 (2008).
17. Z. Ge, S. T. Wu, S. S. Kim, J. W. Park, and S. H. Lee, *Appl. Phys. Lett.* **92**, 181109 (2008).
18. R. Lu, S. T. Wu, and S. H. Lee, *Appl. Phys. Lett.* **92**, 051114 (2008).